Control by interconnection of the Kirchhoff plate within the port-Hamiltonian framework*

Andrea Brugnoli[1] and Daniel Alazard[1] and Valérie Pommier-Budinger[1] and Denis Matignon[1]

***Abstract*— The Kirchhoff plate model is here detailed by using a tensorial port-Hamiltonian (pH) formulation. A structure-preserving discretization of this model is then achieved by using the partitioned finite element (PFEM). This methodology easily accounts for the boundary variables and the finite dimensional system can be interconnected to the surrounding environment in an simple and structured manner. The algebraic constraints to be considered are deduced by the boundary conditions, that may be homogeneous or defined by an interconnection with another dynamical system.**

The versatility of the proposed approach is presented by means of numerical simulations. A first illustration considers a rectangular plate clamped on one side and interconnected to a rigid rod welded to the opposite side. A second example exploits the collocated output feature of pH systems to perform damping injection in a plate undergoing an external forcing. A stability proof is obtained effortlessly as the Hamiltonian is a Lyapunov function.

I. INTRODUCTION

The port-Hamiltonian (pH) framework has proved to be a powerful framework for modeling and control multi-physics system [1]. During the last years distributed systems, i.e. systems ruled by partial differential equations (PDEs) have attracted a lot of interest [2]. The modularity of the pH paradigm is particularly appealing as it provides a structured and coherent way to build complex system. Infinite [3] and finite [4] dimensional pH systems can be connected together giving rise to another pH system.

In order to simulate and control such systems, a finite dimensional representation of the distributed system has to be found and it is convenient to use a discretization procedure that preserves the port-Hamiltonian nature and uses standard libraires. The first attempt to perform a structure-preserving discretization dates back to [5], where the authors proposed a mixed finite element spatial discretization for 1D hyperbolic system. Pseudo-spectral methods were studied in [6]. The prototypical example of hyperbolic systems of two conservation laws was discretized by a weak formulation in [7], leading to a Galerkin numerical approximations. A drawback of these methods is that they require specific implementations and cannot be related to standard numerical methods. An extension of the Mixed finite element method to pH system was proposed in [8]. The main point of this methodology is that the integration by parts to be performed so that the symplectic structure is preserved. Several choice of the boundary control are possible and for this reason this method is referred to as the partitioned finite element method (PFEM). If mixed boundary conditions have to be considered the discretized system is an algebraic differential one (pHDAEs), which can be analyzed by referring to [9], [10].

In this paper the Kirchhoff plate model is presented in a pH fashion. The tensorial calculus is employed in order to clearly identify the skew-symmetric nature of the differential operator. The PFEM methodology is then used to obtain a finite dimensional system. Numerical applications are then carried out using the Firedrake platform [11]. An interconnection along the boundary is presented to model an cantilever plate welded to a rigid bar. This serves just as an example as the methodology may be employed to construct complex systems starting from their basic components. A control application by damping injection follows. The plate is interconnected along part of the boundary with a dissipative system. The Hamiltonian for such an interconnected system is a Lyapunov function, therefore the system will tend to the equilibrium point, i.e. the undeformed configuration.

In section II the Kirchhoff Plate model in strong form as a port-Hamiltonian system is described. In section **??** BLABLA

II. PH FORMULATION OF THE KIRCHOFF PLATE

In this section the classical formulation of the Kirchhoff plate the tensorial pH formulation are recalled.

A. Notations

First, the differential operators needed for the following are recalled. For a scalar field $u : \mathbb{R}^d \rightarrow \mathbb{R}$ the gradient is defined as

$$\mathrm{grad}(u) = \nabla u := \left(\partial_{x_1} u \ldots \partial_{x_d} u\right)^T .$$

For a vector field $\boldsymbol{v} : \mathbb{R}^d \rightarrow \mathbb{R}^d$ the symmetric part of the gradient operator Grad (i. e. the deformation gradient in continuum mechanics) is given by

$$\mathrm{Grad}(\boldsymbol{v}) := \frac{1}{2}\left(\nabla \boldsymbol{v} + \nabla^T \boldsymbol{v}\right).$$

*This work is supported by the project ANR-16-CE92-0028, entitled *Interconnected Infinite-Dimensional systems for Heterogeneous Media*, INFIDHEM, financed by the French National Research Agency (ANR) and the Deutsche Forschungsgemeinschaft (DFG). Further information is available at https://websites.isae-supaero.fr/infidhem/the-project.

[1]Andrea Brugnoli, Daniel Alazard, Valérie Pommier-Budinger and Denis Matignon are with ISAE-SUPAERO, Université de Toulouse, France, 10 Avenue Edouard Belin, BP-54032, 31055 Toulouse Cedex 4 {Andrea.Brugnoli, Daniel.Alazard, Valerie.Budinger, Denis.Matignon}@isae.fr

The Hessian operator of u is then computed as follows

$$\mathrm{Hess}(u) = \mathrm{Grad}(\mathrm{grad}(u)),$$

For a tensor field $\boldsymbol{U} : \mathbb{R}^d \rightarrow \mathbb{R}^{d\times d}$, with elements u_{ij}, the divergence is a vector defined column-wise as

$$\mathrm{Div}(\boldsymbol{U}) = \nabla \cdot \boldsymbol{U} := \left(\sum_{i=1}^{d} \partial_{x_i} u_{ij} \right)_{j=1,\dots,d}.$$

The double divergence of a tensor field $\boldsymbol{U}$ is then a scalar field defined as

$$\mathrm{div}(\mathrm{Div}(\boldsymbol{U})) := \sum_{i,j=1}^{d} \partial_{x_i}\partial_{x_j} u_{ij}.$$

The geometrical dimension of interest in this paper is $d = 2$. In the following vectors (tensor) fields and numerical vectors (matrices) will be denote by a lower (upper) case bold letter. It will be clear by the context which mathematical objects is considered. Furthermore, $\mathbb{S}$ denotes the space of symmetric $d \times d$ tensors (matrices).

B. Kirchhoff Model for Thin Plates

The Kirchhoff Model is a generalization to the 2D case of the Euler-Bernoulli beam model and accounts for the shear deformation. Given an open and connected set $\Omega \in \mathbb{R}^2$, the classical equations for this model ([12]) are

$$\rho h \frac{\partial^2 w}{\partial t^2} = -\mathrm{div}(\mathrm{Div}(\boldsymbol{M})), \tag{1}$$

where ρ is the material density, h is the plate thickness, the scalar w is the vertical displacement and $\boldsymbol{M}$ is the symmetric momenta tensor. This tensor is related to the symmetric curvatures tensor $\boldsymbol{K}$ by the bending rigidity tensor, so that $\boldsymbol{M}_{ij} = \boldsymbol{D}_{ijkl}\boldsymbol{K}_{kl}$. The curvature tensor is defined as

$$\boldsymbol{K} := \mathrm{Grad}(\mathrm{grad}(w)).$$

For an homogeneous isotropic material the components of $\boldsymbol{M}, \boldsymbol{K} \in \mathbb{S}$ are relatedby the relations (x denotes index 1, y index 2)

$$\begin{aligned} m_{xx} &= D\left(\kappa_{xx} + \nu\kappa_{yy}\right), \\ m_{yy} &= D\left(\kappa_{yy} + \nu\kappa_{xx}\right), \\ m_{xy} &= D(1-\nu)\kappa_{xy}, \end{aligned}$$

with ν the Poisson ratio, D the bending module. The kinetic and potential energy density $\mathcal{K}$ and $\mathcal{U}$ read

$$\mathcal{K} = \frac{1}{2}\rho h \left(\frac{\partial w}{\partial t}\right)^2, \quad \mathcal{U} = \frac{1}{2}\boldsymbol{M} : \boldsymbol{K}, \tag{2}$$

where $\boldsymbol{M} : \boldsymbol{K} := \sum_{i,j} m_{ij}\kappa_{ij}$ is the tensor contraction. The Hamiltonian is easily written as

$$H = \int_{\Omega} (\mathcal{K} + \mathcal{U}) \ \mathrm{d}\Omega. \tag{3}$$

C. Tensorial Port-Hamiltonian formulation

In order to rewrite the system as a port-Hamiltonian one, the energy variables have to be selected first. This choice is analogous to that of the pH Euler-Bernoulli beam model [13], but with the complication that the energy variables are of scalar and tensorial nature:

$$\begin{aligned} \alpha_w &= \rho h \frac{\partial w}{\partial t}, && \text{Linear momentum,} \\ \boldsymbol{A}_\kappa &= \boldsymbol{K}, && \text{Curvature tensor.} \end{aligned} \tag{4}$$

The co-energy variables are found by computing the variational derivative of the Hamiltonian

$$\begin{aligned} e_w &:= \frac{\delta H}{\delta \alpha_w} = w_t, && \text{Vertical Velocity,} \\ \boldsymbol{E}_\kappa &:= \frac{\delta H}{\delta \boldsymbol{A}_\kappa} = \boldsymbol{M}, && \text{Momenta tensor,} \end{aligned} \tag{5}$$

where $w_t = \frac{\partial w}{\partial t}$ for compactness. The port-Hamiltonian system is expressed as follows

$$\begin{cases} \dfrac{\partial \alpha_w}{\partial t} &= -\mathrm{div}(\mathrm{Div}(\boldsymbol{E}_\kappa)), \\ \dfrac{\partial \boldsymbol{A}_\kappa}{\partial t} &= \mathrm{Grad}(\mathrm{Grad}(e_w)),, \end{cases} \tag{6}$$

If the variables are concatenated together, the formally skew-symmetric operator J can be highlighted

$$\frac{\partial}{\partial t}\begin{pmatrix} \alpha_w \\ \boldsymbol{A}_\kappa \end{pmatrix} = \underbrace{\begin{bmatrix} 0 & -\mathrm{div} \circ \mathrm{Div} \\ \mathrm{Grad} \circ \mathrm{grad} & 0 \end{bmatrix}}_{\mathcal{J}} \begin{pmatrix} e_w \\ \boldsymbol{E}_\kappa \end{pmatrix}, \tag{7}$$

Remark 1: It can be observed that the interconnection structure given by $\mathcal{J}$ mimics that of the Euler-Bernoulli beam (in one spatial dimension the double divergence and the Hessian reduce to the second derivative).

Theorem 1 ([13]): The adjoint of the double divergence of a tensor $\mathrm{div} \circ \mathrm{Div}$ is $-\mathrm{Grad} \circ \mathrm{grad} = -\mathrm{Hess}$, the opposite of the Hessian operator.

The boundary values can be found by evaluating the time derivative of the Hamiltonian and by applying the Green-Gauss theorem [13].

$$\dot{H} = \int_{\partial\Omega} \left\{ w_t \widetilde{q}_n + \omega_n m_{nn} \right\} \ \mathrm{d}s. \tag{8}$$

where s is the curvilinear abscissa The boundary variable are defined as follows

$$\begin{aligned} &\text{Effetive Shear Force} && \widetilde{q}_n := -\mathrm{Div}(\boldsymbol{E}_\kappa) \cdot \boldsymbol{n} - \frac{\partial m_{ns}}{\partial s}, \\ &\text{Flexural momentum} && m_{nn} := \boldsymbol{E}_\kappa : (\boldsymbol{n} \otimes \boldsymbol{n}), \end{aligned} \tag{9}$$

where $m_{ns} := \boldsymbol{E}_\kappa : (\boldsymbol{s} \otimes \boldsymbol{n})$ is the torsional momentum and $\boldsymbol{u} \otimes \boldsymbol{v}$ denotes the outer product of vectors equivalent to a matrix given by $\boldsymbol{u}\boldsymbol{v}^T$. Vectors $\boldsymbol{n}$ and $\boldsymbol{s}$ designate the normal and tangential unit vector to the boundary. The corresponding power conjugated variables are

$$\begin{aligned} &\text{Vertical velocity} && w_t := e_w, \\ &\text{Flexural rotation} && \omega_n := \frac{\partial e_w}{\partial n}. \end{aligned} \tag{10}$$

III. Structure preserving discretization

In this section the structure preserving discretization, that consists of three steps, is detailed:

1) put the system in weak form;
2) perform integrations by parts to get the boundary control of choice;
3) select the finite element spaces to achieve a finite dimensional system.

A. Weak Form

In order to put the system into weak form the first line of (7) is multiplied by v_w (multiplication by a scalar), the second line one by $\boldsymbol{V}_\kappa$ (tensor contraction).

$$\int_\Omega v_w \frac{\partial \alpha_w}{\partial t} \; \mathrm{d}\Omega = - \int_\Omega v_w \mathrm{div}(\mathrm{Div}(\boldsymbol{E}_\kappa)) \; \mathrm{d}\Omega, \tag{11}$$

$$\int_\Omega \boldsymbol{V}_\kappa : \frac{\partial \boldsymbol{A}_\kappa}{\partial t} \; \mathrm{d}\Omega = + \int_\Omega \boldsymbol{V}_\kappa : \mathrm{Grad}(\mathrm{grad}(e_w)) \; \mathrm{d}\Omega, \tag{12}$$

For sake of simplicity, all test and unknown functions can be collected in one variable

$$v := (v_w, \boldsymbol{V}_\kappa), \qquad \alpha := (\alpha_w, \boldsymbol{A}_\kappa), \qquad e := (e_w, \boldsymbol{E}_\kappa), \tag{13}$$

so that the previous system is rewritten compactly as

$$\left(v, \frac{\partial \alpha}{\partial t}\right) = (v, \mathcal{J} e), \tag{14}$$

where the bilinear form $(v, u) = \int v \cdot u \; \mathrm{d}\Omega$, is the inner product on space $\mathscr{L}^2(\Omega) := L^2(\Omega) \times L^2(\Omega; \mathbb{S})$. The operator $\mathcal{J}$ was defined in equation (7). It can be decomposed into the sum of three operators

$$\mathcal{J} = \mathcal{J}_{\mathrm{divDiv}} + \mathcal{J}_{\mathrm{Hess}}, \tag{15}$$

where $\mathcal{J}_{\mathrm{divDiv}}, \mathcal{J}_{\mathrm{Hess}}$ contain only the double divergence (divDiv) and Hessian operator respectively.

The integration by part has to be performed so that the final bilinear form on the right-hand side remains skew-symmetric. Obviously, since $\mathcal{J}$ is skew-symmetric $\mathcal{J}_{\mathrm{divDiv}} = -\mathcal{J}_{\mathrm{Hess}}^*$, where A^* is the formal adjoint of operator A. Depending on which of the two differential operators is chosen for the integration by parts, two different boundary controls can arise [13] (other choices are possible but less meaningful under a physical point of view).

B. Boundary control through forces and momenta

Applying the integration by parts twice on $\mathcal{J}_{\mathrm{divDiv}}$ is integrated by parts (meaning that the right-hand side of equation (11) is integrated by parts twice) then

$$(v, Je) = j_{\mathrm{Hess}}(v, e) + f_N(v), \tag{16}$$

where now the bilinear form

$$j_{\mathrm{Hess}}(v, e) = (\mathcal{J}_{\mathrm{divDiv}}^* v, e) + (v, \mathcal{J}_{\mathrm{Hess}} e)$$

is skew symmetric and can be expressed as follows

$$\begin{aligned} j_{\mathrm{Hess}}(v, e) := & - \int_\Omega \mathrm{Grad}(\mathrm{grad}(v_w)) : \boldsymbol{E}_\kappa \; \mathrm{d}\Omega \, \mathrm{d}s \\ & + \int_\Omega \boldsymbol{V}_\kappa : \mathrm{Grad}(\mathrm{grad}(e_w)) \; \mathrm{d}\Omega. \end{aligned} \tag{17}$$

The linear functional $f_N(v)$ represents the boundary term associated with forces and momenta. The subscript N denotes the fact that classical Neumann conditions appear as boundary input. It reads

$$f_N(v) = \int_{\partial\Omega} \left\{ v_w \widetilde{q}_n + v_{\omega_n} m_{nn} \right\} \; \mathrm{d}s, \tag{18}$$

where $v_{\omega_n} = \frac{\partial v_w}{\partial n}$. In this first case, the boundary controls $\boldsymbol{u}_\partial$ and the corresponding output $\boldsymbol{y}_\partial$ are

$$\boldsymbol{u}_\partial = \begin{pmatrix} \widetilde{q}_n \\ m_{nn} \end{pmatrix}_{\partial\Omega}, \qquad \boldsymbol{y}_\partial = \begin{pmatrix} w_t \\ \omega_n \end{pmatrix}_{\partial\Omega}.$$

C. Finite Dimensional System

In this subsection the formulation (16) is used is order to explain the discretization procedure and the associated finite elements.

a) Discretization Procedure: Test and co-energy variables are discretized using the same basis function (Galerkin Method)

$$\begin{aligned} v_w &= \sum_{i=1}^{N_w} \phi_w^i(x, y) \, v_w^i, & e_w &= \sum_{i=1}^{N_w} \phi_w^i(x, y) \, e_w^i(t), \\ \boldsymbol{V}_\kappa &= \sum_{i=1}^{N_\kappa} \boldsymbol{\Phi}_\kappa^i(x, y) \, v_\kappa^i, & \boldsymbol{E}_\kappa &= \sum_{i=1}^{N_\kappa} \boldsymbol{\Phi}_\kappa^i(x, y) \, e_\kappa^i(t), \end{aligned} \tag{19}$$

The basis function $\phi_w^i, \boldsymbol{\Phi}_\kappa^i \in \mathbb{S}$, have to be chosen in a suitable function space $\mathcal{V}^h$ in the domain of operator $\mathcal{J}$, i.e. $\mathcal{V}^h \subset \mathcal{V} \in \mathcal{D}(\mathcal{J})$. The discretized skew-symmetric bilinear form given in (17) then reads

$$\boldsymbol{J}_d = \begin{bmatrix} 0 & -\boldsymbol{D}_{\mathrm{H}}^T \\ \boldsymbol{D}_{\mathrm{H}} & 0 \end{bmatrix}, \tag{20}$$

where $\boldsymbol{A}^T$ is the transpose of the $\boldsymbol{A}$ matrix. The matrix $\boldsymbol{D}_{\mathrm{H}}$ is computed in the following way

$$\boldsymbol{D}_{\mathrm{H}}(i, j) = \int_\Omega \boldsymbol{\Phi}_\kappa^i : \mathrm{Grad}(\mathrm{grad}(\phi_w^j)) \, \mathrm{d}\Omega, \quad \in \mathbb{R}^{N_\kappa \times N_w}, \tag{21}$$

where $A(i, j)$ indicates the entry in the matrix corresponding to the i th row and j th column. The energy variables are deduced from the co-energy variables

$$\alpha_w = \rho h e_w, \qquad \boldsymbol{A}_\kappa = \boldsymbol{D}^{-1} \boldsymbol{E}_\kappa. \tag{22}$$

The symmetric bilinear form on the left side of (16) is discretized as $\boldsymbol{M}_{\mathrm{pl}} = \mathrm{diag}[\boldsymbol{M}_w, \, \boldsymbol{M}_\kappa]$ with

$$\begin{aligned} \boldsymbol{M}_w(i, j) &= \int_\Omega \rho h \, \boldsymbol{\phi}_w^i \, \boldsymbol{\phi}_w^j \; \mathrm{d}\Omega \; \in \mathbb{R}^{N_w \times N_w}, \\ \boldsymbol{M}_\kappa(i, j) &= \int_\Omega \left(\boldsymbol{D}^{-1} \boldsymbol{\Phi}_\kappa^i \right) : \boldsymbol{\Phi}_\kappa^j \; \mathrm{d}\Omega \; \in \mathbb{R}^{N_\kappa \times N_\kappa}, \end{aligned} \tag{23}$$

To deal with generic boundary conditions the Lagrange multipliers have to be introduced in (18)

$$\lambda_{\widetilde{q}_n} = \sum_{i=1}^{N_{\widetilde{q}_n}} \boldsymbol{\phi}_{\widetilde{q}_n}^i(s) \lambda_{\widetilde{q}_n}^i, \quad \lambda_{m_{nn}} = \sum_{i=1}^{N_{m_{nn}}} \boldsymbol{\phi}_{m_{nn}}^i(s) \lambda_{m_{nn}}^i, \tag{24}$$

If inhomogeneous Neumann boundary conditions are then discretized as

$$\widetilde{q}_n = \sum_{i=1}^{N_{\widetilde{q}_n}} \phi^i_{\widetilde{q}_n}(s)\, \widetilde{q}^i_n, \qquad m_{nn} = \sum_{i=1}^{N_{m_{nn}}} \phi^i_{m_{nn}}(s)\, m^i_{nn}. \tag{25}$$

It is now possible to construct the following constraints and input matrices

$$\begin{aligned}
\boldsymbol{G}_w(i,j) &= \int_{\Gamma_C \cup \Gamma_S} \phi^i_w\, \phi^j_{\widetilde{q}_n}\, \mathrm{d}s, \quad \in \mathbb{R}^{N_w \times N_{\widetilde{q}_n}}, \\
\boldsymbol{B}_{\widetilde{q}_n}(i,j) &= \int_{\Gamma_{\widetilde{q}_n}} \phi^i_w\, \phi^j_{\widetilde{q}_n}\, \mathrm{d}s, \quad \in \mathbb{R}^{N_w \times N_{\widetilde{q}_n}}, \\
\boldsymbol{G}_{\omega_n}(i,j) &= \int_{\Gamma_C} \frac{\partial \phi^i_w}{\partial n}\, \phi^j_{m_{nn}}\, \mathrm{d}s, \quad \in \mathbb{R}^{N_w \times N_{m_{nn}}}, \\
\boldsymbol{B}_{m_{nn}}(i,j) &= \int_{\Gamma_{m_{nn}}} \frac{\partial \phi^i_w}{\partial n}\, \phi^j_{m_{nn}}\, \mathrm{d}s, \quad \in \mathbb{R}^{N_w \times N_{m_{nn}}},
\end{aligned} \tag{26}$$

where Γ_C, Γ_S are subsets of the boundary where clamped and simply supported boundary conditions apply and $\Gamma_{\widetilde{q}_n}, \Gamma_{m_{nn}}$ are subsets where inhomogeneous Neumann conditions hold. Defining the matrices

$$\boldsymbol{G}_D = \begin{bmatrix} \boldsymbol{G}_w & \boldsymbol{G}_{\omega_n} \\ \boldsymbol{0} & \boldsymbol{0} \end{bmatrix}, \qquad \boldsymbol{B}_N = \begin{bmatrix} \boldsymbol{B}_{\widetilde{q}_n} & \boldsymbol{B}_{m_{nn}} \\ \boldsymbol{0} & \boldsymbol{0} \end{bmatrix},$$

the final port-Hamiltonian descriptor system (pHDAEs), as defined in [9], is written as

$$\begin{gathered}
\begin{bmatrix} \boldsymbol{M}_{\text{pl}} & \boldsymbol{0} \\ \boldsymbol{0} & \boldsymbol{0} \end{bmatrix} \frac{\mathrm{d}}{\mathrm{d}t} \begin{pmatrix} \boldsymbol{e}_{\text{pl}} \\ \boldsymbol{\lambda}_D \end{pmatrix} = \begin{bmatrix} \boldsymbol{J}_d & \boldsymbol{G}_D \\ -\boldsymbol{G}_D^T & \boldsymbol{0} \end{bmatrix} \begin{pmatrix} \boldsymbol{e}_{\text{pl}} \\ \boldsymbol{\lambda}_D \end{pmatrix} + \begin{bmatrix} \boldsymbol{B}_N \\ \boldsymbol{0} \end{bmatrix} \boldsymbol{u}, \\
\boldsymbol{y} = \begin{bmatrix} \boldsymbol{B}_N^T & \boldsymbol{0} \end{bmatrix} \begin{pmatrix} \boldsymbol{e}_{\text{pl}} \\ \boldsymbol{\lambda}_D \end{pmatrix}
\end{gathered} \tag{27}$$

where $\boldsymbol{e}_{\text{pl}} = (\boldsymbol{e}_w; \boldsymbol{e}_\kappa)$, $\boldsymbol{\lambda}_D = (\boldsymbol{\lambda}_{\widetilde{q}_n}; \boldsymbol{\lambda}_{m_{nn}})$ are column-wise (denoted by ;) concatenation of the co-energy variables, Lagrange multipliers. The input $\boldsymbol{u} = (\widetilde{\boldsymbol{q}}_n; \boldsymbol{m}_{nn})$ are the known Neumann conditions (boundary forces and momenta) at the boundary. The subscript N, D refer to Neumann and Dirichlet boundary conditions.

b) Finite Element Choice: The domain of the operator $\mathcal{J}$ in (7) is $\mathcal{D}(J) = H^2(\Omega) \times H^{\text{div Div}}(\Omega, \mathbb{R}^{2\times 2}_{\text{sym}}) +$ boundary conditions. For this reason a suitable choice for the functional space is

$$(v_w, \boldsymbol{V}_\kappa) \in H^2(\Omega) \times H^2(\Omega, \mathbb{R}^{2\times 2}_{\text{sym}}) \equiv \mathscr{H}, \tag{28}$$

since $\mathscr{H} \subset \mathcal{D}(J)$.

Remark 2: It has to be appointed that the space $H^{\text{div Div}}(\Omega, \mathbb{R}^{2\times 2}_{\text{sym}})$ was never addressed in the mathematical literature. For this reason the only way to deal with this problem numerically is to use $H^2(\Omega)$ conforming finite elements.

The Firedrake library [11] was used to implement the numerical analysis as it provides functionalities to automate the generalized mappings for H^2 conforming finite elements (like the Hermite, Bell or Argyris finite elements). All the variables, i.e. the velocity e_w and the momenta tensor $\boldsymbol{E}_\kappa$ as well as the corresponding test functions, are discretized by the same finite element space, the Bell finite element [14], denoted by $H^2_r(\mathbb{P}_5, \Omega)$. The multipliers are therefore discretized by using second degree Lagrange polynomials defined over the boundary and denoted with $H^1_r(\mathbb{P}_2, \partial\Omega)$.

IV. Interconnection with a finite dimensional conservative pH system

In this section the interconnection of an infinite and finite port system is explained in both the infinite and finite dimensional setting. This paradigm, here illustrated by means of an example, provides an easy way to construct arbitrarily complex system given its basic components. Infinite and finite dimensional can be coupled together, making it possible to construct models for complex applications.

A. Infinite dimensional setting

Consider an infinite dimensional pH system (or distributed pH system, dpH) and a finite dimensional pH system denoted by equations

$$\text{pH} \begin{cases} \dot{\boldsymbol{x}}_2 = \boldsymbol{J} \dfrac{\partial H_2}{\partial \boldsymbol{x}_2} + \boldsymbol{B}\boldsymbol{u}_2 \\ \boldsymbol{y}_2 = \boldsymbol{B}^T \dfrac{\partial H_2}{\partial \boldsymbol{x}_2} + \boldsymbol{D}\boldsymbol{u}_2 \end{cases}, \tag{29}$$

$$\text{dpH} \begin{cases} \dfrac{\partial x_1}{\partial t} = \mathcal{J} \dfrac{\delta H_1}{\delta x_1} \\ u_{\partial,1} = \mathcal{B} \dfrac{\delta H_1}{\delta x_1}, \\ y_{\partial,1} = \mathcal{C} \dfrac{\delta H_1}{\delta x_1} \end{cases} \tag{30}$$

where $\boldsymbol{x} \in \mathbb{R}^n, \boldsymbol{u}, \boldsymbol{y} \in \mathbb{R}^m$ $x_1 \in \mathscr{X}$ and $u_{\partial,1} \in \mathscr{U}$, $y_{\partial,1} \in \mathscr{Y} = \mathscr{U}'$ belong to some Hilbert spaces (the prime denotes the dual of a space) and $\mathcal{B} : \mathscr{X} \to \mathscr{U}$, $\mathcal{C} : \mathscr{X} \to \mathscr{Y}$ are boundary operators. The duality pairings for the boundary ports are then denoted by

$$\langle u_{\partial,1},\, y_{\partial,1} \rangle_{\mathscr{U}\times\mathscr{Y}}, \qquad \langle \boldsymbol{u}_2,\, \boldsymbol{y}_2 \rangle_{\mathbb{R}^m}.$$

Given a compact interconnection operator $\mathcal{W} : \mathscr{Y} \to \mathbb{R}^m$ consider the following power preserving interconnection

$$\boldsymbol{u}_2 = -\mathcal{W}\, y_{\partial,1}, \qquad u_{\partial,1} = \mathcal{W}^*\, \boldsymbol{y}_2, \tag{31}$$

where $\mathcal{W}^*$ denotes the adjoint of $\mathcal{W}$. As an illustration, a rigid rod welded to the plate is considered. A rigid rod can be written undergoing small displacements about the z axis and small rotation about the x axis can be written as port-Hamiltonian in co-energy variables system with structure

$$\begin{gathered}
\begin{bmatrix} M & 0 \\ 0 & J_G \end{bmatrix} \frac{d}{dt} \begin{pmatrix} v_G \\ \theta_G \end{pmatrix} = \begin{pmatrix} F_z \\ T_x \end{pmatrix} = \boldsymbol{u}_{\text{rod}}, \\
\boldsymbol{y}_{\text{rod}} = \begin{pmatrix} v_G \\ \theta_G \end{pmatrix},
\end{gathered} \tag{32}$$

with v_G, θ_G, J_G the linear velocity, angular velocity and rotary inertia about G, the center of mass, M the total mass and F_z, T_x the force along z and the torque along x. The Hamiltonian reads $H_{\text{rod}} = \frac{1}{2}\left(M_G v_G^2 + J_G \theta_G^2\right)$. The rod is welded to a rectangular thin plate of sides L_x, L_y on side $x = L_x$. The boundary variables for the plate involved in the interconnection are

$$u_{\partial,\text{pl}} = w_t(x = L_x, y), \qquad y_{\partial,\text{pl}} = \widetilde{q}_n(x = L_x, y).$$

The space $\mathscr{Y}$ is the space of square-integrable functions on with support $\Gamma_{\text{int}} = \{(x, y) |\ x = L_x, 0 \leq y \leq L_y\}$. The compact interconnection operator then reads

$$\mathcal{W} y_{\partial,\text{pl}} = \int_{\Gamma_{\text{int}}} \begin{pmatrix} y_{\partial,\text{pl}} \\ y_{\partial,\text{pl}}\,(y - L_y/2) \end{pmatrix} \mathrm{d}s. \tag{33}$$

The adjoint operator is then obtained considering that $\boldsymbol{u}_{\text{rod}} = \mathcal{W} y_{\partial,\text{pl}}$ and that the inner product of $\mathbb{R}^m$ is easily converted to an inner product on the space $L^2(\Gamma_{\text{int}})$ (square-integrable functions on Γ_{int})

$$\begin{aligned} \langle \mathcal{W} y_{\partial,\text{pl}},\ \boldsymbol{y}_{\text{rod}} \rangle_{\mathbb{R}^m} &= \langle \mathcal{W}^* \boldsymbol{y}_{\text{rod}},\ y_{\partial,\text{pl}} \rangle_{L^2(\Gamma_{\text{int}})}\,, \\ \mathcal{W}^* \boldsymbol{y}_{\text{rod}} &= v_G + \theta_G\,(y - L_y/2)\,. \end{aligned}$$

The interconnection (31) will assure that the two components are connected in a power preserving manner.

B. Finite dimensional setting

Consider a rectangular plate of side L_x, L_y, clamped at $x = 0$ and welded to a rigid rod on $x = L_x$. The discretized system 27 is now modified to take into account the presence of an inhomogeneous Dirichlet boundary condition, i.e the input needed for the interconnection. It reads

$$\begin{aligned} \begin{bmatrix} \boldsymbol{M}_{\text{pl}} & \boldsymbol{0} \\ \boldsymbol{0} & \boldsymbol{0} \end{bmatrix} \begin{pmatrix} \dot{\boldsymbol{e}}_{\text{pl}} \\ \dot{\boldsymbol{\lambda}}_D \end{pmatrix} &= \begin{bmatrix} \boldsymbol{J}_d & \boldsymbol{G}_D \\ -\boldsymbol{G}_D^T & \boldsymbol{0} \end{bmatrix} \begin{pmatrix} \boldsymbol{e}_{\text{pl}} \\ \boldsymbol{\lambda}_D \end{pmatrix} + \begin{bmatrix} \boldsymbol{0} \\ \boldsymbol{B} \end{bmatrix} \boldsymbol{u}_{\text{pl}}, \\ \boldsymbol{y}_{\text{pl}} &= \begin{bmatrix} \boldsymbol{0} & \boldsymbol{B}^T \end{bmatrix} \begin{pmatrix} \boldsymbol{e}_{\text{pl}} \\ \boldsymbol{\lambda}_D \end{pmatrix}. \end{aligned} \tag{34}$$

Here the Lagrange multipliers and associated matrices $\boldsymbol{\lambda}_D = (\boldsymbol{\lambda}_{\Gamma_C};\ \boldsymbol{\lambda}_{\Gamma_{\text{int}}})$, $\boldsymbol{G}_D = [\boldsymbol{G}_{\Gamma_C},\ \boldsymbol{G}_{\Gamma_{\text{int}}}]$, $\boldsymbol{B} = [\boldsymbol{0};\ \boldsymbol{I}]$ are split between the homogeneous and non-homogeneous Dirichlet boundary conditions. The rigid rod is written compactly

$$\begin{aligned} \boldsymbol{M}_{\text{rod}} \dot{\boldsymbol{e}}_{\text{rod}} &= \boldsymbol{u}_{\text{rod}}, \\ \boldsymbol{y}_{\text{rod}} &= \boldsymbol{e}_{\text{rod}}, \end{aligned} \tag{35}$$

where $\boldsymbol{e}_{\text{rod}} = (v_G\ \ \theta_G)$, $\boldsymbol{M}_{\text{rod}} = \text{diag}(M_G,\ J_G)$. The interconnection matrix if obtained once the operator $\mathcal{W}^*$ is put into weak form

$$\begin{aligned} \boldsymbol{W}^T(i, j) &= \left\langle \boldsymbol{\phi}_{\widetilde{q}_n}^i,\ \mathcal{W}^* \boldsymbol{\phi}_{\mathbb{R}^2}^j \right\rangle_{L^2(\Gamma_{\text{int}})} \\ &= \int_{\Gamma_{\text{int}}} [\boldsymbol{\phi}_{\widetilde{q}_n}^i,\ \boldsymbol{\phi}_{\widetilde{q}_n}^i (y - L_y/2)]\ \mathrm{d}s, \end{aligned}$$

where $\boldsymbol{\phi}_{\mathbb{R}^2}^j,\ \forall j = 1, 2$ is the canonical basis for $\mathbb{R}^2$. The final system is obtained considering the power preserving interconnection $\boldsymbol{u}_{\text{rod}} = -\boldsymbol{W} \boldsymbol{y}_{\text{pl}},\ \boldsymbol{u}_{\text{pl}} = \boldsymbol{W}^T \boldsymbol{y}_{\text{rod}}$ is then the augmented system

$$\boldsymbol{E}_{\text{aug}} \dot{\boldsymbol{x}}_{\text{aug}} = \boldsymbol{J}_{\text{aug}} \boldsymbol{x}_{\text{aug}}, \tag{36}$$

with $\boldsymbol{x}_{\text{aug}} = (\boldsymbol{e}_{\text{pl}}, \boldsymbol{e}_{\text{rod}}, \boldsymbol{\lambda}_D)$ and

$$\boldsymbol{E}_{\text{aug}} = \begin{bmatrix} \boldsymbol{M}_{\text{pl}} & \boldsymbol{0} & \boldsymbol{0} \\ \boldsymbol{0} & \boldsymbol{M}_{\text{rod}} & \boldsymbol{0} \\ \boldsymbol{0} & \boldsymbol{0} & \boldsymbol{0} \end{bmatrix},\ \boldsymbol{J}_{\text{aug}} = \begin{bmatrix} \boldsymbol{J}_d & \boldsymbol{0} & \boldsymbol{G}_D \\ \boldsymbol{0} & \boldsymbol{0} & \boldsymbol{G}_{\text{rod}} \\ -\boldsymbol{G}_D^T & -\boldsymbol{G}_{\text{rod}}^T & \boldsymbol{0} \end{bmatrix}, \tag{37}$$

with $\boldsymbol{G}_{\text{rod}} = -\boldsymbol{B}^T \boldsymbol{W}$. Distributed forces are easily accounted for.

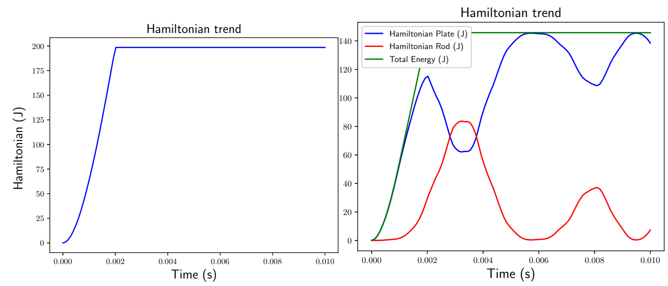

(a) Without rod (b) With rod

Fig. 1: Simulation results for the network.

Plate Parameters		Simulation Settings	
E	$70\ [GPa]$	Δt	$0.001\ [ms]$
ν	0.35	Integrator	Störmer-Verlet
h/L	0.05	N° Elements	4
$L_x = L_y$	$1\ [m]$	FE space	Bell ($\boldsymbol{e}_{\text{pl}}$) $\times$ CG^2 ($\boldsymbol{\lambda}$)

TABLE I: Simulations settings and parameters

C. Numerical Simulation

To validate the approach numerical simulations considering system (37) were carried out. A final time equal to $t_{\text{end}} = 10[ms]$ is taken. A vertical distributed force given by expression

$$\boldsymbol{f}_w = \begin{cases} 10^5 \left[y + 10\,(y - L_y/2)^2\right] [Pa], & \forall\, t < 0.2\, t_{\text{end}}, \\ 0, & \forall\, t \geq 0.2\, t_{\text{end}}, \end{cases}$$

acts on the plate. The rigid rod has mass $M = 50\,[kg]$ and length $L_{\text{rod}} = 1[m]$. The plate parameters and settings for the discretization (a uniform grid is taken) ar provided in table I. The constraints are eliminated considering the projection matrix

$$\boldsymbol{P}_\lambda = \boldsymbol{I} - \boldsymbol{G} \left(\boldsymbol{G}^T \boldsymbol{M}^{-1} \boldsymbol{G}\right) \boldsymbol{G}^T \boldsymbol{M}^{-1}$$

with $\boldsymbol{M} = \text{diag}(\boldsymbol{M}_{\text{pl}},\ \boldsymbol{M}_{\text{rod}})$, $\boldsymbol{G} = [\boldsymbol{G}_D;\ \boldsymbol{G}_{\text{rod}}]$.

Snapshots of simulations without and with the rigid rod are reported in figures 2, 3. The deformations undergone by the plate are clear affected by the presence of the rod: the maximum deformation as well as the Hamiltonian value, once the excitation is removed, are lower. The interconnected side remains straight along the whole simulation, meaning that the constraints are respected.

V. Damping Injection

The damping injection technique allows to asymptotically stabilize and infinite dimensional system. It relies on the La Salle invariance principle ([1] chapter 6, proposition 6.2). Starting from system (27)

VI. Conclusion

The conclusion goes here.

Acknowledgment

The authors would like to thank Michel Salaün, Xavier Vaisseur and Ghislain Haine from ISAE-SUPAERO for their insightful observations and comments.

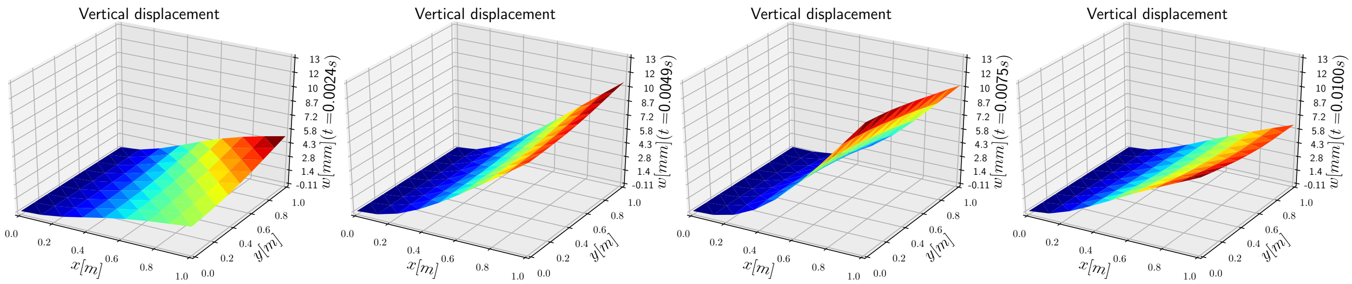

(a) $t = 0.25\ t_{\text{end}}$ (b) $t = 0.5\ t_{\text{end}}$ (c) $t = 0.75\ t_{\text{end}}$ (d) $t = t_{\text{end}}$

Fig. 2: Snapshots without rod ($t_{\text{end}} = 10\,[ms]$).

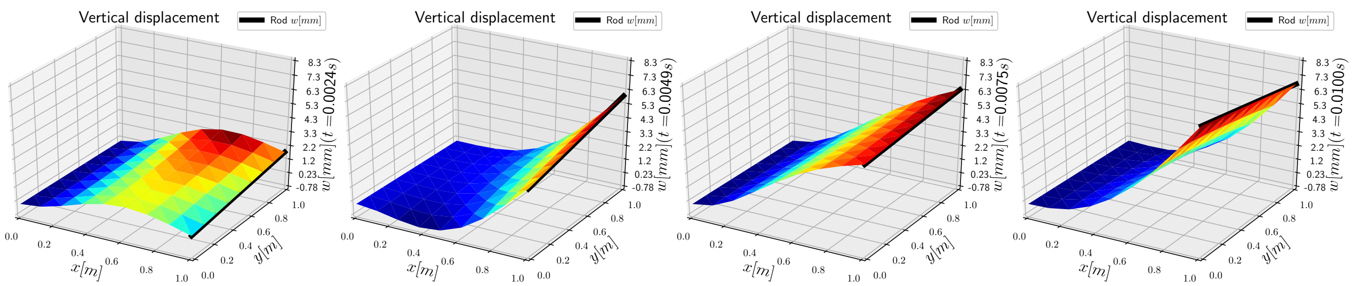

(a) $t = 0.25\ t_{\text{end}}$ (b) $t = 0.5\ t_{\text{end}}$ (c) $t = 0.75\ t_{\text{end}}$ (d) $t = t_{\text{end}}$

Fig. 3: Snapshots with rod ($t_{\text{end}} = 10\,[ms]$).

References

[1] V. Duindam, A. Macchelli, S. Stramigioli, and H. Bruyninckx, *Modeling and Control of Complex Physical Systems*. Springer Verlag, 2009.

[2] B. Jacob and H. Zwart, *Linear Port-Hamiltonian Systems on Infinite-*

dimensional Spaces, ser. Operator Theory: Advances and Applications. Germany: Springer Verlag, 2012, no. 223.

[3] M. Kurula, H. Zwart, A. J. van der Schaft, and J. Behrndt, "Dirac structures and their composition on Hilbert spaces," *Journal of mathematical analysis and applications*, vol. 372, no. 2, pp. 402–422, 2010, 10.1016/j.jmaa.2010.07.004.

[4] J. Cervera, A. J. van der Schaft, and A. Baños, "Interconnection of port-Hamiltonian systems and composition of Dirac structures," *Automatica*, vol. 43, no. 2, pp. 212–225, feb 2007.

[5] G. Golo, V. Talasila, A. J. van der Schaft, and B. Maschke, "Hamiltonian discretization of boundary control systems," *Automatica*, vol. 40, no. 5, pp. 757–771, May 2004.

[6] R. Moulla, L. Lefevre, and B. Maschke, "Pseudo-spectral methods for the spatial symplectic reduction of open systems of conservation laws," *Journal of Computational Physics*, vol. 231, no. 4, pp. 1272–1292, 2012.

[7] P. Kotyczka, B. Maschke, and L. Lefvre, "Weak form of Stokes-Dirac structures and geometric discretization of port-Hamiltonian systems," *Journal of Computational Physics*, vol. 361, pp. 442 – 476, 2018.

[8] F. L. Cardoso-Ribeiro, D. Matignon, and L. Lefèvre, "A structure-preserving partitioned finite element method for the 2d wave equation," in *6th IFAC Workshop on Lagrangian and Hamiltonian Methods for Nonlinear Control*, Valparaíso, CL, 2018, pp. 1–6.

[9] C. Beattie, V. Mehrmann, H. Xu, and H. Zwart, "Linear port-Hamiltonian descriptor systems," *Mathematics of Control, Signals, and Systems*, vol. 30, no. 4, p. 17, 2018.

[10] A. J. van der Schaft, "Port-Hamiltonian differential-algebraic systems," in *Surveys in Differential-Algebraic Equations I*. Berlin, Heidelberg: Springer Berlin Heidelberg, 2013, pp. 173–226.

[11] M. Homolya and D. A. Ham, "A parallel edge orientation algorithm for quadrilateral meshes," *SIAM Journal on Scientific Computing*, vol. 38, no. 5, pp. S48–S61, 2016.

[12] S. Timoshenko and S. Woinowsky-Krieger, *Theory of plates and shells*, ser. Engineering societies monographs. McGraw-Hill, 1959.

[13] A. Brugnoli, D. Alazard, V. Budinger, and D. Matignon, "Port-Hamiltonian formulation and symplectic discretization of plate models. Part II : Kirchhoff model for thin plates," 2018, arXiv preprint:1809.11136, Under Revision.

[14] K. Bell, "A refined triangular plate bending finite element," *International Journal for Numerical Methods in Engineering*, vol. 1, no. 1, pp. 101–122, 1969.